

# Binary Mixtures in Linear Convection Arrays

Pulak K. Ghosh,<sup>\*,[a]</sup> Yuxin Zhou,<sup>[b]</sup> Yunyun Li,<sup>[b]</sup> Fabio Marchesoni,<sup>\*,[b, c]</sup> and Franco Nori<sup>[d, e]</sup>

We numerically investigated the dynamics of a mixture of finite-size active and passive disks in a linear array of two-dimensional convection rolls. The interplay of advection and steric interactions produces a number of interesting effects, like the stirring of a passive colloidal fluid by a small fraction of slow active particles, or the separation of the mixture active and

passive colloidal fractions by increasing the motility of the active one, which eventually clusters in stagnation areas along the array walls. These mechanisms are quantitatively characterized by studying the dependence of the diffusion constants of the active and passive particles on the parameters of the active mixture fraction.

## Introduction

Brownian motion in convective laminar flows<sup>[1]</sup> is a topic of interdisciplinary research for its applications to transport phenomena at large<sup>[2,3]</sup> and small scales.<sup>[4,5]</sup> For instance, under quite general conditions, advection has been proven, both analytically<sup>[6–9]</sup> and experimentally,<sup>[10–12]</sup> to enhance the diffusion of passive colloidal particles along a linear array of convection rolls. This is a combined effect of thermal noise and advection. Indeed, a noiseless particle would keep circulating inside the convection roll where it had been injected.<sup>[13]</sup>

Active particles in a linear convection array behave differently. An active particle is modeled as a particle propelling itself with tunable constant speed and direction changing because of collisions with obstacles and other particles, or the torque associated with the convective flow, or fluctuations (either of the suspension fluid or the self-propulsion mechanism).<sup>[14–17]</sup> A slow active particle ends up trapped in a convection roll as long as the fluctuations affecting its dynamics are negligible,<sup>[18]</sup> whereas a fast active particle tends to sojourn against the array walls, in the stagnation areas separating the convection rolls. In the latter regime, the particle diffusion along the array is dominated by the self-propulsion mechanism.<sup>[19,20]</sup>

So far, all studies on the advection-diffusion of colloidal suspension in convection arrays were conducted in the low-density regime, namely, they focused on the diffusion of a

single particle. Of course, the dynamics of a suspension of Brownian particles is in itself a well established topic due to its applications in colloids and aerosols science.<sup>[21]</sup> Weakly attracting colloidal particles<sup>[22]</sup> are known to cluster into a variety of continuously time-evolving structures, ranging from dimers to crystals.<sup>[23,24]</sup> Most remarkably, in the context of soft matter, clustering of overdamped active particles in a stationary suspension fluid can occur even in the absence of particle attraction, because the particles on the cluster surface point mostly inwards.<sup>[25,26]</sup> Under the same conditions, steric interactions do not suffice to make passive particles cluster; their distribution would remain uniform at all times. However, despite the wide literature on colloidal suspensions, the impact of collisions on particle transport in a convection array has been addressed only recently.<sup>[27]</sup> Extensive numerical simulations showed,<sup>[28]</sup> for instance, that particle-particle collisions allow convection cell crossings by noiseless particles (active and passive, alike) and, therefore, athermal diffusion in convection arrays and turbulent flows at large.

In this paper we investigate the collisional effects in a binary mixture made of colloidal particles of the same size, one species active and the other one passive. As mentioned above, single active and passive particles advected in a linear convection array exhibit different diffusion properties. On the other hand, steric collisions, due to the particle finite size, allow the two mixture fractions to interact, so that the question arises about the advection-diffusion of a binary mixture. To avoid unnecessary numerical complications, we restrict our study to planar convective flows and particles are modeled by hard disks. Our numerical simulations reveal a number of interesting new features, like the strong stirring action exerted on a passive colloidal fluid by a small fraction of slow active particles, or the separation of the mixture into two distinct colloidal fluids for strong self-propulsion of the active fraction, the passive fluid circulating inside the convection rolls and the active one accumulating in stagnation areas along the array walls.

To emphasize the interplay of advection and steric collisions, we neglected two further aspects of the colloidal fluid dynamics, namely hydrodynamical and inertial effects. Laminar flows around finite-size particles are likely to affect the advective drag of the suspension fluid;<sup>[29–31]</sup> therefore, the conclusions of the present paper should be reconsidered at


[a] P. K. Ghosh  
Department of Chemistry, Presidency University, Kolkata 700073, India  
E-mail: pulak.chem@presiuniv.ac.in

[b] Y. Zhou, Y. Li, F. Marchesoni  
Center for Phononics and Thermal Energy Science, Shanghai Key Laboratory of Special Artificial Microstructure Materials and Technology, School of Physics Science and Engineering, Tongji University, Shanghai 200092, China

[c] F. Marchesoni  
Dipartimento di Fisica, Università di Camerino, I-62032 Camerino  
E-mail: fabio.marchesoni@pg.infn.it

[d] F. Nori  
Theoretical Quantum Physics Laboratory, RIKEN Cluster for Pioneering Research, Wako-shi, Saitama 351-0198, Japan.

[e] F. Nori  
Physics Department, University of Michigan, Ann Arbor, Michigan 48109-1040, USA.

 An invited contribution to the Special Collection featuring the Theoretical Chemistry Symposium 2021

high packing fractions. Inertia in colloid advection is also a well-established problem,<sup>[32,33]</sup> unavoidable in the case of massive particles. However, neglecting both effects can be appropriate at low Reynolds numbers, when one deals with nano- and micro-particles,<sup>[4]</sup> as is often the case in soft matter systems.

The contents of this paper is organized as follows. First, we introduce the key ingredients of a two-dimensional (2D) model of an advected overdamped binary mixture consisting of active and passive hard disks of the same size, namely, the fluid streaming function, the particle-particle interaction function, and the self-propulsion mechanism of the active fraction. Known results holding in the low-density (single particle) regime are summarized in section. Non-interacting Colloidal Particles in a Convection Array. In the next section, One-Component Suspensions, we show that particle collisions are responsible for spatial inhomogeneities in pure passive and active suspensions confined into a linear convection array. In section Binary Mixtures we investigate the interaction between the active and passive components of the mixture. The stirring effects of a small fraction of slow active particles (Section Stirring) and the active-passive separation caused by fast active particles (Section Demixing) are discussed in detail. In section Diffusion in a Binary Mixture, the diffusion of the passive and active particles are compared under both stirring and demixing conditions. In the last section, we draw a few concluding remarks in view of future work.

## Model

Following Ref. [9], we model a 2D linear convection array as a stationary laminar flow with stream function,<sup>[32,33]</sup>

$$\psi(x, y) = (U_0 L / 2\pi) \sin(2\pi x / L) \sin(2\pi y / L), \quad (1)$$

periodic in the longitudinal  $x$  direction and confined in the transverse direction,  $0 \leq y \leq L/2$ . The two parallel walls,  $y = 0$  and  $y = L/2$ , act as dynamical reflecting boundaries. The unit cell of the stream function consists of two counter-rotating convection rolls, see Figure 1, with advection velocity field  $\vec{v}_\psi = (\partial_y, -\partial_x)\psi$ . The flow parameters (the spatial period,  $L$ , and the advection speed,  $U_0$ ) can be combined<sup>[9]</sup> to define the advection diffusion scale,  $D_L = U_0 L / 2\pi$ , and the roll vorticity,  $\Omega_L = 2\pi U_0 / L$ .

We simulated a colloidal suspension consisting of a mixture of  $N$  hard disks per unit cell, including a fraction  $\eta$  of active disks. All disks, active and passive alike, repel each other with a potential function modeled by the truncated-shifted Lennard-Jones function,<sup>[34]</sup>

$$V_{ij} = 4\epsilon \left[ \left( \frac{\sigma}{r_{ij}} \right)^{12} - \left( \frac{\sigma}{r_{ij}} \right)^6 \right], \quad \text{if } r_{ij} \leq r_m \\ = 0 \text{ otherwise,} \quad (2)$$

where  $r_m = 2^{1/6}\sigma$  and  $\sigma$  represents the effective particle "diameter". Since our conclusions turn out to be rather insensitive to the interaction strength parameter,  $\epsilon = v_\epsilon \sigma^2 / 24$ ,

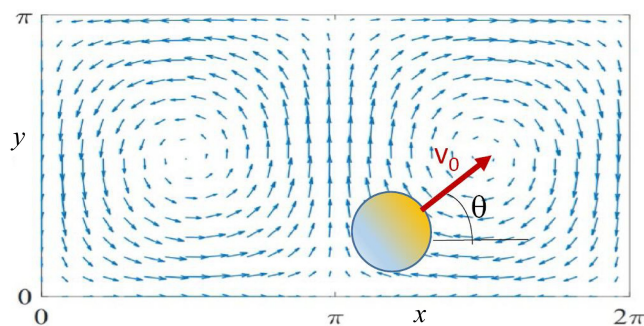


**Figure 1.** Advection flow field,  $\vec{v}_\psi$ , in a linear convection array with the periodic stream function  $\psi(x, y)$  of Eq. (1). The unit cell is delimited by horizontal reflecting walls,  $y = 0$  and  $y = L/2$ , and periodic vertical boundaries,  $x = 0$  and  $x = L$ , with  $L = 2\pi$ . The self-propelling particle of Eq. (3) is sketched for reader's convenience.

we set  $v_\epsilon = 1$  throughout the present numerical study.<sup>[27]</sup> This choice implies that particles interact only through steric repulsion, i.e., all hydrodynamical interactions will be neglected. Some important effects due to the actual geometry of the particles and the self-propulsion mechanism can be encoded in the model parameters.<sup>[17]</sup> Extensions of this model are also possible.<sup>[35,36]</sup>

As we are interested in colloidal mixtures at very low Reynolds numbers, the dynamics of the  $i$ -th disk will be modeled by an overdamped (massless) active Brownian particle (ABP) governed by two translational and one rotational Langevin equation (LE),

$$\begin{aligned} \dot{\vec{r}}_i &= \vec{v}_{L,i} + \vec{v}_{\psi,i} + \vec{v}_{0,i} + \sqrt{D_0} \xi_i(t) \\ \dot{\theta}_i &= (\alpha/2) \nabla \times \vec{v}_{\psi,i} + \sqrt{D_\theta} \xi_{\theta,i}(t), \end{aligned} \quad (3)$$

where  $i, j = 1, \dots, N$ , and  $\vec{r}_i = (x_i, y_i)$ . Here,  $\vec{v}_{\psi,i}$  is the advection velocity introduced above, and  $\vec{v}_{L,i} = -\sum_{j=1}^N \nabla_i V_{ij}$  is the collisional term due to pair repulsion. For an active particle, the self-propulsion vector,  $\vec{v}_{0,i} = v_0(\cos\theta_i, \sin\theta_i)$  has constant modulus,  $v_0$ , and is oriented at an angle  $\theta_i$  with respect to horizontal axis  $x$ . Of course, for a passive particle,  $\vec{v}_{0,i} = 0$ . The flow shear exerts a torque on the active particles proportional to the local fluid vorticity,  $\nabla \times \vec{v}_\psi$ .<sup>[18,19]</sup> For simplicity, we adopt Faxén's second law, which, for an ideal no-stick spherical particle, yields  $\alpha = 1$ .<sup>[37]</sup> Of course, no shear torque is exerted on a symmetric passive particles with  $v_0 = 0$ .

The translational thermal noises in the  $x$  and  $y$  directions,  $\xi_i(t) = (\xi_{x,i}(t), \xi_{y,i}(t))$ , for all particles, and the rotational noise,  $\xi_{\theta,i}(t)$ , for the active particles only, are stationary, independent, delta-correlated Gaussian noises,  $\langle \xi_{\mu,i}(t) \xi_{\nu,j}(0) \rangle = 2\delta_{ij} \delta_{\mu,\nu} \delta(t)$ , with  $\mu, \nu = x, y, \theta$ .  $D_0$  and  $D_\theta$  are the respective noise strengths, which for generality we assume to be statistically unrelated.<sup>[38]</sup>

The LE (3) can be conveniently reformulated in dimensionless units by rescaling  $(x, y) \rightarrow (\tilde{x}, \tilde{y}) = (2\pi/L)(x, y)$  and  $t \rightarrow \tilde{t} = \Omega_L t$ . After rescaling, the tunable model parameters read  $\sigma \rightarrow (2\pi/L)\sigma$ ,  $v_\epsilon \rightarrow v_\epsilon/U_0$ ,  $v_0 \rightarrow v_0/U_0$ ,  $D_0 \rightarrow D_0/D_L$  and  $D_\theta \rightarrow D_\theta/\Omega_L$ . Alternatively, upon setting  $L = 2\pi$  and  $U_0 = 1$ , our

simulation results can be regarded as expressed in dimensionless units, and then scaled back to arbitrary dimensional units. The stochastic differential Eqs. (3) for  $D_0 > 0$  and/or  $D_\theta > 0$ , were numerically integrated by means of a standard Milstein scheme.<sup>[39]</sup> Particular caution was exerted in the noiseless regime,  $D_0 = 0$ , because transients can grow exceedingly long, thus affecting the computation of both the long-time spatial distribution of the mixture in the array and the diffusion constants  $D_{a,p} = \lim_{t \rightarrow \infty} \langle [x(t) - x(0)]^2 \rangle_{a,p} / 2t$ , respectively of the active and passive particles, with the stochastic average,  $\langle \dots \rangle_{a,p}$ , taken over the relevant mixture component.

### Non-interacting Colloidal Particles in a Convection Array

Colloidal dynamics in convective flows has been studied (analytically and numerically) mostly ignoring particle interactions.<sup>[6–9,13,19]</sup> A 2D fluid of passive particles in a convection array was first investigated in Ref. [27] under the simplifying assumption that non-steric interactions might be neglected. Particle collisions were shown to affect the colloidal fluid dynamics well beyond the low density (single particle) approximation.

For this reason, we recall now the main properties of the diffusive dynamics of a *single* overdamped colloidal particle in a convection array:

- (i) In the absence of translational noise,  $D_0 = 0$ , an advected noiseless passive particle gets trapped inside a single convection roll, where it keeps retracing the same closed orbit, depending on its injection point.<sup>[2,32]</sup>
- (ii) In sharp contrast, for  $D_0 > 0$  the spatial distribution of a passive Brownian particle along the convection rolls is uniform. Moreover, the translational noise activates particle hopping between adjacent rolls with average hopping time inversely proportional to  $D_0$ .<sup>[13]</sup>
- (iii) Accordingly, a *passive* Brownian particle undergoes normal diffusion along the array with diffusion constant  $D \sim \sqrt{D_L D_0}$ , where in our notation  $D_0$  coincides with its free diffusion constant in the suspension fluid at rest, and  $D_L$  is the characteristic advection diffusion constant defined above.<sup>[6–9]</sup> At high Péclet numbers,  $D_0 \ll D_L$ , advection enhances the spatial diffusion of the particle by pushing it along the roll boundary layers.<sup>[10–12]</sup>
- (iv) Advection also favors the confinement of noiseless *active* particles. A noiseless active particle,  $D_0 = D_\theta = 0$ , ends up being trapped in a convection roll, unless its speed is raised above a certain threshold value,  $v_{th}$ , proportional to the fluid advection speed,  $U_0$ .<sup>[18]</sup> For  $v_0 > v_{th}$  the particle trajectory can be either bounded (but not necessarily closed) or unbounded. Spatial diffusion of an advected active particle as a combined effect of rotational and thermal fluctuations has been investigated in Refs. [19, 20] (see Section One-component suspensions, for details relevant to the present report).
- (v) The action of upward flows may suffice to counter the effect of a downward transverse bias, for instance, of gravitational settling. Suppose a suspended passive particle

moves under the action of the external term,  $-g\hat{e}$  with  $\hat{e} = (0, 1)$  and  $g > 0$ , to be inserted on the r.h.s. of the first LE (3). In the noiseless regime,  $D_0 = 0$ , the probability the particle gets trapped in the cells of a 2D convection array (periodic in both the  $x$  and  $y$  direction) depends on the ratio  $g/U_0$ —fully trapped for  $g/U_0 = 0$  and no trapping for  $g/U_0 = 1$ .<sup>[32,33]</sup> On the contrary, in the presence of translational noise, its spatial distribution remains uniform. In linear convection arrays the confining walls modify the spatial distribution of an advected colloidal fluid, active and passive,<sup>[20,40]</sup> alike, as reported in the foregoing section.

Our numerical simulations confirmed that particle collisions play an important role in the dynamics of an advected suspension, which led us to reconsider some of the above results.

### One-Component Suspensions

In the context of soft matter, it has been reported that clustering of overdamped active particles in a *stationary* suspension fluid can occur even in the absence of particle attraction.<sup>[25,26]</sup> In sharp contrast, under the same conditions, finite-size passive particles would not cluster (that is, not as an effect of steric interactions, only); consistently with the single-particle picture, the suspension distribution would remain uniform at all times.

In a convective flow, a passive colloidal suspension behaves differently.<sup>[27]</sup> The spatial configuration of an initially uniform suspension of hard disks advected in a linear convection array is displayed in Figure 2 [and 4(a)] for increasing values of its density  $2N/L^2$  (or average packing fraction  $\phi = \pi\sigma^2 N/2L^2$ ). After a long running time, say  $t = 10^5$ , the particles have diffused toward the center of the convection rolls, where they form stable rotating patterns, ranging from micellar patterns at low  $N$ , to compact clusters at high  $N$ . Clusters consist of a lattice core surrounded by ring-like formations and a dilute gas of strongly advected particles in the vicinity of the cell boundaries. As detailed in Ref. [27], the clustering process of a passive colloidal fluid inside the convection rolls is governed by the inter-particle collisions.

The clustering dynamics illustrated in Figure 2 is independent of the suspension preparation (not reported), but extremely sensitive to translational noise with  $D_0 > 0$ . This result is consistent with the earlier observation that, inside a convection roll, under periodic boundary conditions, a single Brownian tracer approaches a uniform spatial distribution.<sup>[13,18]</sup>

The behavior of a suspension of  $N$  self-propelling disks in a linear convection array is illustrated in Figure 3. The difference with the same density passive suspension of Figure 2 is apparent. As already reported for a single active ABP,<sup>[41]</sup> the disks, after reaching the channel walls, tend to slide along them until they accumulate in the stable stagnation areas, namely at the base of the ascending and descending flows, respectively against the lower and upper walls. Such accumulation areas are centered at  $(x, y) = (L/2, 0)$  and  $(0, L/2)$ , with  $x$  given mod( $L/2$ ).

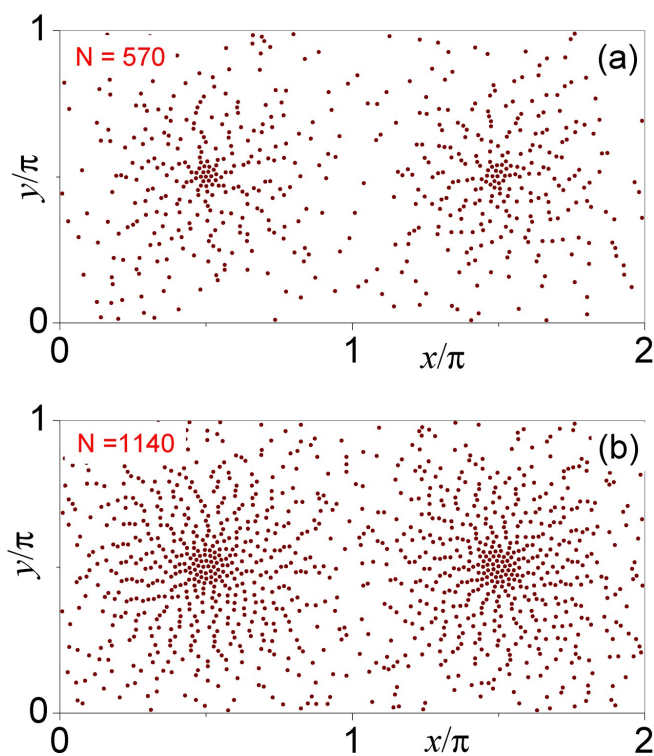


**Figure 2.** Clustering of a suspension of noiseless passive particles,  $D_0 = v_0 = 0$ , after a running time  $t = 10^5$ . At  $t = 0$  the suspension was uniformly distributed with  $N$  particles per unit cell of Figure 1. Other simulation parameters are:  $\sigma = 0.05$ ,  $v_e = 1$ ,  $L = 2\pi$  and  $U_0 = 1$ .

Contrary to the case of a single ABP,<sup>[41]</sup> steric interactions bring the disks in the stagnation areas to an almost complete rest, the fraction of the floating disks decreasing with increasing  $v_0$ . This behavior is apparent when self-propulsion wins over advection, that is for  $v_0/U_0 > 1$ . Lowering  $v_0$  for  $v_0 < U_0$ , the disk accumulation along the channels walls diminishes, as most of the disks are dragged along by the convective flow. Contrary to the passive suspension of Figure 2, here the advected disks seem to form small, short-lived clusters, which can be interpreted as a residual effect of the athermal clustering effect reported in Ref. [25]. Advection disrupts the clustering action associated with self-propulsion; clustering of slow active disks can only be achieved at much higher packing fractions than in the absence of advection.

## Binary Mixtures

Binary mixtures made of different active species have been the subject of extensive numerical and analytical investigations for at least a decade now.<sup>[42–52]</sup> The attention of most researchers focused on the phenomenon known as motility induced phase separation (MIPS), whereby the mixture components tends to separate as an effect of their motility difference.<sup>[42,43]</sup> Phase separation can occur on either local or global scales, with the formation of one-species clusters of various size. Clustering is initiated by the confining action exerted by the active

particles.<sup>[25,26,53–55]</sup> However, MIPS is sensitive to other aspects of the microscopic mixture dynamics, like hydrodynamical and phoretic effects,<sup>[44,56,57]</sup> chemical interactions,<sup>[45]</sup> particle geometry,<sup>[46]</sup> and external confining fields of force,<sup>[47]</sup> to mention but a few. In the absence of these additional factors, MIPS emerges from a delicate balance between steric interactions (the phase packing fractions) and self-propulsion (their motility). Not surprisingly, this phenomenon has been investigated for mixtures diffusing in equilibrium suspension fluids and mostly in the absence of geometric constraints.<sup>[48]</sup>

In the following we will study phase aggregation and segregation of an active-passive binary mixture advected in a linear convection array.

## Stirring

Consider a suspension of noiseless passive particles in the convection array of Eq. (1). We know from Section One-component suspensions that for not too small packing fractions the particles tend to aggregate in regular patterns rotating around the center of the convection rolls. Assume now to add a small amount of slow active particles with the same geometry, and ask ourselves what is their impact on the dynamics of the passive fluid.

We simulated numerically this situation for a mixture of  $N = 3420$  disks in Figure 4, where the self-propelling disks have speed  $v_0 = 0.1 U_0$ . An active fraction as small as  $\eta = 0.01$ , panel (b), suffices to destroy the clustering pattern of the pure passive suspension, panel (a). As a result, for  $\eta = 0.05$  the passive particles circulate inside the convection rolls with almost uniform spatial distribution. Mixture stirring by active swimmers is a well-known mechanism,<sup>[51]</sup> here, it can be invoked to mimic the effects of a tunable translational noise.

On further increasing the active fraction,  $\eta$ , the distributions of both phases undergo micro-clustering. For  $\eta = 0.5$ , panel (d), both species aggregate in small, short-lived clusters. This effect is clearly due to the behavior of the active component of the mixture reported in Section One-component suspensions. Note that the suspension of Figure 3(a) is the same as the mixture in Figure 4 but for  $\eta = 1$ . Moreover, the emerging micro-clusters are made of active and passive particles; no phase separation was detected on the cluster scales, as long as the self-propulsion speed was kept sufficiently low.

## Demixing

On increasing the speed,  $v_0$ , of the active disks, the scenario changes dramatically, as illustrated in Figure 5 for low and high values of the active fraction, respectively,  $\eta = 0.1$  and  $\eta = 0.5$ . The micro-clustering phenomenon disappears for  $v_0/U_0 \gtrsim 0.3$ . Similarly to the pure active suspension of Figure 3, for  $v_0 \gtrsim U_0$  self-propulsion wins over advection, and the active disk pile up in the stagnation areas at the base of the ascending (descending) flows against the lower (upper) array walls. As a result, the passive disks, separated from the active ones, diffuse back

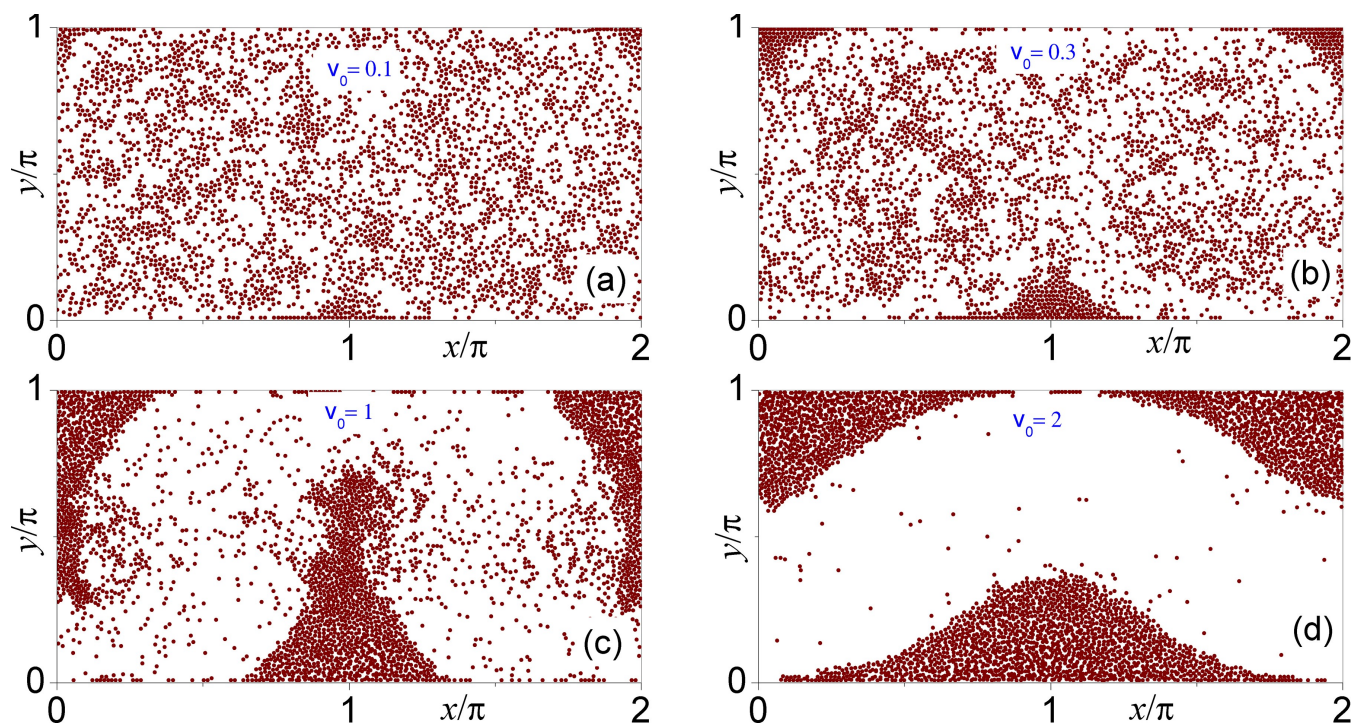


**Figure 3.** Spatial distribution of a suspension of  $N = 3420$  noiseless active particles,  $D_0 = 0$ , with increasing speeds,  $v_0$  (see legend), after a running time  $t = 10^5$ . At  $t = 0$  the suspension was uniformly distributed with  $N$  particles per unit cell of Figure 1. Other simulation parameters are:  $D_\theta = 0.01$ ,  $\sigma = 0.05$ ,  $v_\varepsilon = 1$ ,  $L = 2\pi$  and  $U_0 = 1$ .

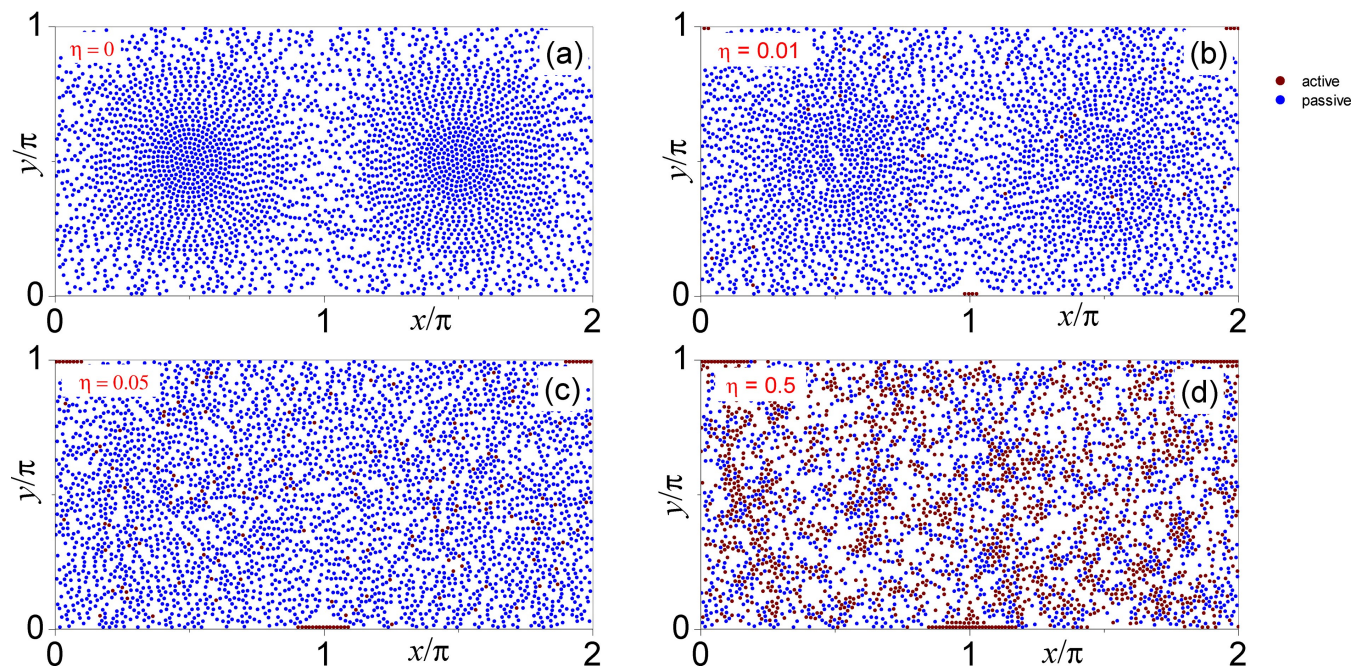


**Figure 4.** Binary mixture of active (blue) and passive disks with  $D_0 = 0$ ,  $D_\theta = 0.01$  and  $v_0 = 0.1$  at  $t = 10^5$ .  $N = 3420$  is the total number of disks, and  $\eta$  (see legends) the active fraction. At  $t = 0$  all  $N$  disks were randomly distributed in the  $\psi(x, y)$  unit cell of Figure 1. All other simulation parameters are as in Figure 2.

toward the center of the convection rolls, regrouping in dynamical patterns, as first reported in Ref. [27], see also Figure 2.

Phase demixing grows more effective with increasing  $v_0$ , its onset being retarded at large  $\eta$ . A large packing fraction of active disks is harder to be contained in the stagnation areas

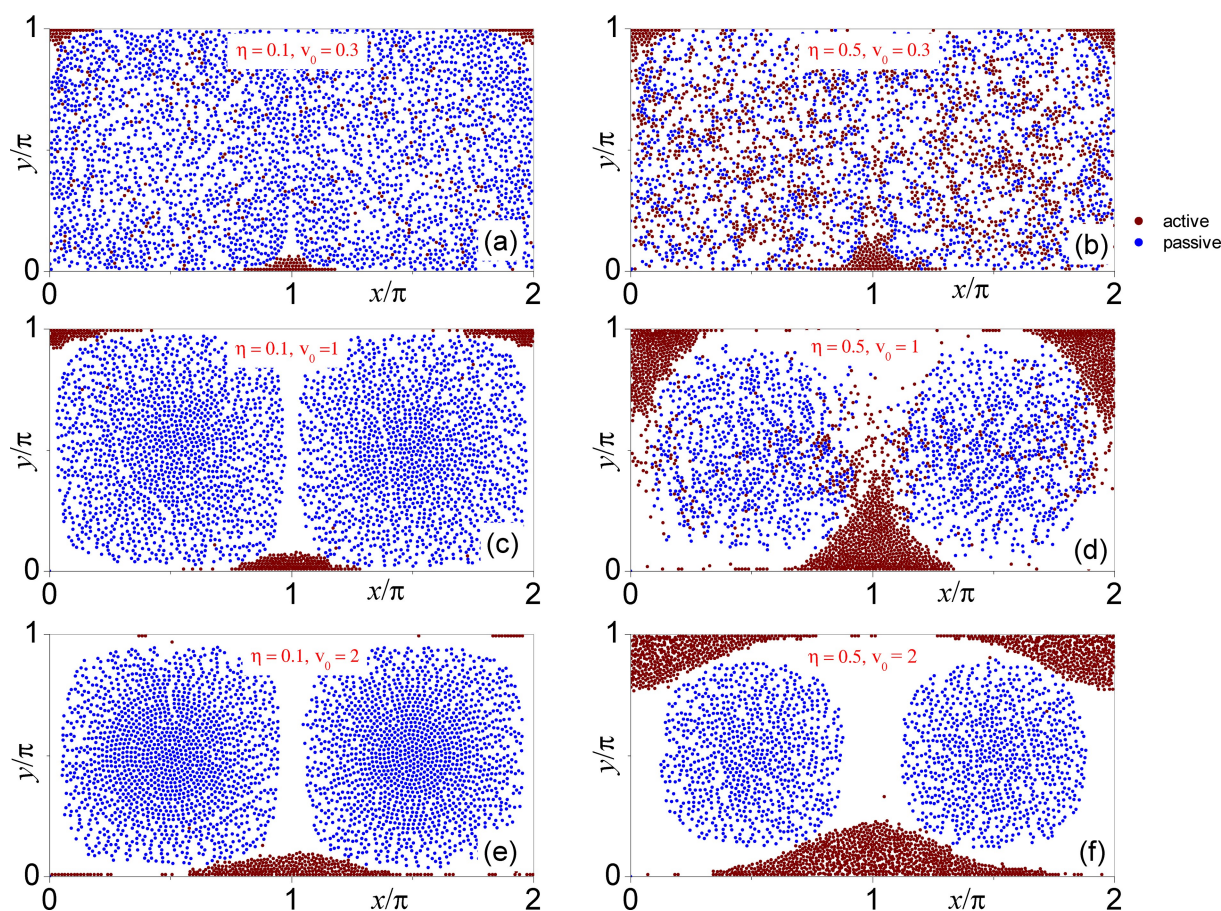


**Figure 5.** Binary mixture of  $N = 3420$  active (blue) and passive disks (brown) with  $D_0 = 0$ ,  $D_\theta = 0.01$  and  $v_0 = 0.3, 1.0$  and  $2.0$  (from top to bottom): (a)–(c)  $\eta = 0.1$  and (d)–(f)  $\eta = 0.5$ . At  $t = 0$  all  $N$  disks were randomly distributed in the  $\psi(x, y)$  unit cell of Figure 1; all snapshots were taken at  $t = 10^5$ . All other simulation parameters are as in Figure 2.

separating the convection rolls; hence the “fountain effect” in Figures 3(c) and 5(e). This explains why more active disks keep circulating inside the convection rolls for  $\eta = 0.5$  than  $\eta = 0.1$ , compare panels (b) and (e). Demixing is complete only for  $v_0 \gg U_0$ . However, even then, a small number of active disks still happens to switch array wall. These are the disks stuck in the outer layers of the aggregates grown along the walls. Owing to the rotational fluctuation with time constant  $D_\theta^{-1}$ , they can self-propel toward the center of the channel, thus crossing the passive fluid circulating inside the convection rolls. Traces of their passage are clearly visible as “scars” in the otherwise regular patterns of the separated passive phase.

## Diffusion in a Binary Mixture

We already mentioned that pair collisions in a colloidal fluid of appropriate density suffice to make an individual particle cross the convection roll separatrices even in the absence of thermal noise and self-propulsion. As reported in Ref. [27], the particles of a noiseless passive suspension may thus diffuse along a linear convection array as an effect of steric collision alone (athermal diffusion). On the other hand, advection hinders the

phenomenon of athermal clustering that takes place in dense active suspensions under no-flow conditions.<sup>[25,26]</sup> Not surprisingly, in a binary mixture the interplay between active and passive phases affects the diffusion of both species.

## Passive Particles

The numerical characterization of the athermal diffusion of the passive phase of a binary mixture of  $N = 1140$  disks is illustrated in Figure 6. The mean-square displacement (MSD<sub>p</sub>) of the passive disks grows asymptotically with normal diffusion law,  $\Delta x^2(t) = \langle [x(t) - x(0)]^2 \rangle_p = 2D_p t$ , for any choice of the tunable model parameters. The dependence of  $D_p$  on the self-propulsion speed of the active mixture fraction,  $v_0$ , is plotted in panel (c) for different values of  $\eta$ , and, vice versa, its dependence on  $\eta$  for different values of  $v_0$ , in the inset of panel (b).

For  $v_0 = 0$ , the mixture is a passive fluid with  $\eta = 0$  and its diffusion is purely athermal.<sup>[27]</sup> In the opposite limit,  $v_0 \gg U_0$ , the active phase accumulates against the array walls, leaving the passive one largely undisturbed. The passive particles then form regular patterns that rotate around the center of the convection rolls; the area accessible to them is restricted to the

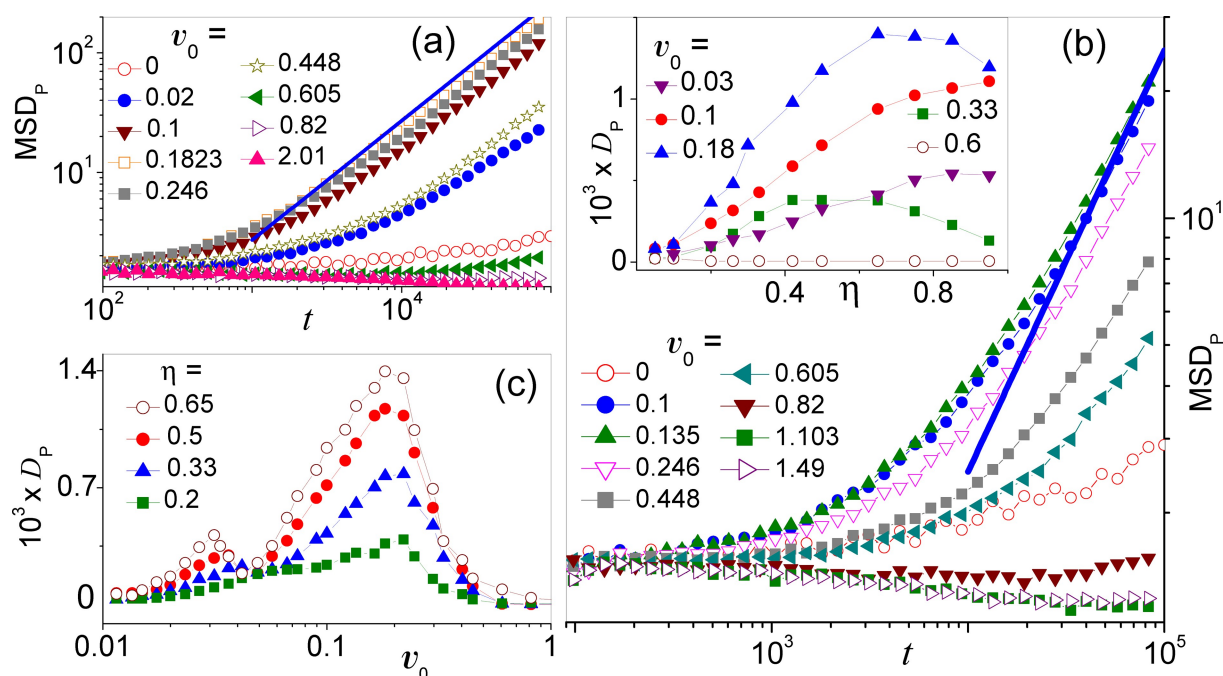


**Figure 6.** Mean-square displacement,  $\text{MSD}_p = \langle [x(t) - x(0)]^2 \rangle_p$ , vs. time,  $t$ , of the passive disks in a binary mixture of  $N = 1140$  disks along the convection array of Figure 1 for different self-propulsion speeds,  $v_0$ , and (a)  $\eta = 0.5$  and (b)  $\eta = 0.1$ . The relevant diffusion constants,  $D_p$ , are plotted vs.  $v_0$  for different  $\eta$  in (c) and vs.  $\eta$  for different  $v_0$  in the inset of (b). The asymptotic normal diffusion power-law is represented by solid lines. Other simulation parameters are:  $D_0 = 0$ ,  $D_\sigma = 0.01$ ,  $\sigma = 0.05$ ,  $v_\varepsilon = 1$ ,  $L = 2\pi$  and  $U_0 = 1$ .

sinusoidal effective channel delimited by the lateral aggregates of active particles. This suppresses the diffusion of the passive mixture fraction almost completely, as apparent in Figures 6(a),(b) for  $v_0 \gtrsim U_0$ . Such an effect grows more prominent on increasing the active fraction  $\eta$ .

Adding slow active disks to a passive suspension favours its diffusivity. Accordingly, the curves of  $D_p$  versus  $v_0$ ,  $D_p(v_0)$ , exhibit two maxima, a smaller one for  $v_0/U_0 \simeq 0.03$  and a higher one for  $v_0/U_0 \simeq 0.2$ . We attribute such optimal diffusive regimes to two distinct mechanisms; (i) the first  $D_p$  peak is a signature of the stirring effect introduced in sub-section stirring, whereby the motility of the active disks destroys the dynamical clusters of the passive disks localized at the center of the convection rolls, thus favoring their diffusion along the array; (ii) the higher peak is related to the formation of micro-clusters, with active and passive disks clumping together into short-lived small-scale structures. The higher motility of the active phase is thus transferred to the passive one, whose diffusivity is thus enhanced.<sup>[52]</sup>

The maxima of the curves  $D_p(v_0)$  have a distinct dependence on the fraction,  $\eta$ , of the active mixture component, see inset of Figure 6(b). The height of the smaller  $D_p$  peak increases monotonically with  $\eta$ , which suggests that the slow active disks stir the mixture independently of each other, i.e., not through a collective action. The position of the higher  $D_p$  peak,  $v_0 \simeq 0.2$ , is not sensitive to  $\eta$ , but its height goes through a maximum for  $\eta \simeq 0.7$ . We associate this diffusion peak with the breaking up of the circulation of the active mixture fraction inside the convection rolls. Due to the steric interactions, the active

particles diffuse toward the outer boundaries of the convection rolls and get advected parallel to the array walls.<sup>[19,20]</sup> In the process they drag along the passive particles, whose diffusion is thus greatly enhanced. However, this is no longer the case for larger values of  $v_0$  (and  $\eta$ ), when the active phase tends to separate from the passive one, by aggregating against the walls.

### Active Particles

The different diffusion regimes of the passive component of the mixture have a clear-cut signature in the  $v_0$  dependence of the active diffusion constant,  $D_a$ , displayed in Figure 7 for different values of the active fraction,  $\eta$ . For  $v_0 \leq 0.2$ ,  $D_a$  is quite insensitive to the density of the active disks, panel (a), and grows linearly with  $v_0$ , panel (b), as already observed for a single active particle in Ref. [19]. The curves of panel (a) also show that increasing  $\eta$  favors first the depinning of the active disks from the convection rolls, signalled by an increase of  $D_a$ , and then their aggregation in the appropriate stagnation areas along the channels walls, with a consequent drop of  $D_a$ .

The relation between the  $v_0$  dependence of  $D_a$  and  $D_p$  becomes apparent when comparing Figures 6(c) and 7(b). The growth of the diffusion constant of a single active particle in a convection array is known to turn from linear to quadratic,<sup>[19]</sup> as suggested in Figure 7(b). In the presence of steric interactions, however two dips appear in the  $D_a(v_0)$  curves: (i) one in correspondence with the higher maximum of  $D_p(v_0)$ , which can

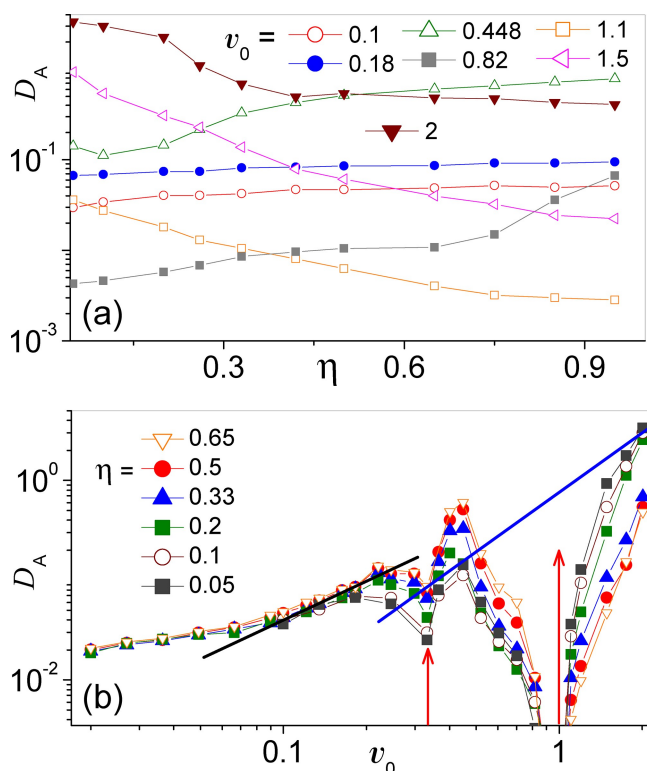


**Figure 7.** Diffusion constant,  $D_a$ , of the active disks of the binary mixture of Figure 6: (a) vs.  $\eta$  for different  $v_0$ ; (b) vs.  $v_0$  for different  $\eta$ . The vertical arrows in (b) correspond to the higher maxima of the curves  $D_p(v_0)$  in Figure 6(c) (left) and the single-particle depinning condition from the wall advective flow,  $v_0 = U_0$  (right). Straight lines are linear and quadratic reference power-laws.

be attributed to the “diffusivity transfer”<sup>[52]</sup> between the active and passive mixture components; (ii) a deeper one for  $v_0 \simeq U_0$ , which marks the aggregation of the fast active disks at the bases of the ascending (descending) flows along the lower (upper) array walls. The active disks resume their typical motility with  $D_a \propto v_0^2$  only for much larger self-propulsion speeds, when the advection effects grow negligible.

## Conclusions

We have investigated the diffusion properties of a mixture of active and passive colloidal particles of finite size advected in a linear convection array. The combination of advection and steric collisions results in peculiar mixing and demixing mechanisms, which depend on the motility and density of the active fraction.

Besides its fundamental interest in the field of soft and biological matter, this problem has practical implications, for instance, in medical sciences.<sup>[58–60]</sup> Let us consider a convection flow along a narrow channel, say, the vessel of a biological organism. The particles advected by the flow can be either passive drug complexes or active swimmers (synthetic or biological, alike), or a mixture thereof. Based on the outcome of the present study, a small fraction of active nano-particles can

help control drug delivery by preventing the passive suspension from clustering in the convection rolls. Vice versa, an excess of more motile active swimmers tends to sediment in stagnation areas against the channel walls, thus causing solid occlusions that may hinder transport in the channel.

As the focus of this report was on the interplay of advective and collisional dynamics, two important ingredients were ignored, namely, inertia and hydrodynamical interactions. While this assumption may be justified at low Reynolds numbers, appreciable inertial and hydrodynamical effects are expected in the case of large and massive advected particles, irrespective of their motility. This question will be addressed in a forthcoming publication.

## Acknowledgements

We thank RIKEN Hokusai for providing computational resources. P.K.G. is supported by SERB Core Research Grant No. CRG/2021/007394. Y.L. is supported by the NSF China under grants No. 11875201 and No.11935010. F.N. is supported in part by: Nippon Telegraph and Telephone Corporation (NTT) Research, the Japan Science and Technology Agency (JST) [via the Quantum Leap Flagship Program (Q-LEAP), and the Moonshot R&D Grant Number JPMJMS2061], the Japan Society for the Promotion of Science (JSPS) [via the Grants-in-Aid for Scientific Research (KAKENHI) Grant No. JP20H00134], the Army Research Office (ARO) (Grant No. W911NF-18-1-0358), the Asian Office of Aerospace Research and Development (AOARD) (via Grant No. FA2386-20-1-4069), and the Foundational Questions Institute Fund (FQXi) via Grant No. FQXi-IAF19-06.

## Conflict of Interest

The authors declare no conflict of interest.

## Data Availability Statement

The data that support the findings of this study are available on request from the corresponding author. The data are not publicly available due to privacy or ethical restrictions.

**Keywords:** Active particles · convection rolls · diffusion · clustering · phase-separation

- [1] H. K. Moffatt, G. M. Zaslavsky, P. Comte, M. Tabor Tabor (Eds.), *Topological Aspects of the Dynamics of Fluids and Plasmas*(Springer Netherlands, 1992).
- [2] S. Chandrasekhar, *Hydrodynamic and Hydromagnetic Stability*(Oxford University Press, New York, 1967).
- [3] S. Childress, *Phys. Earth Planet. Inter.* **1979**, *20*, 172–180.
- [4] B. J. Kirby, *Micro- and Nanoscale Fluid Mechanics: Transport in Microfluidic Devices*(Cambridge University Press, 2010).
- [5] X. Yang, C. Liu, Y. Li, F. Marchesoni, P. Hänggi, H. P. Zhang, *Proc. Natl. Acad. Sci. USA* **2017**, *114*, 9564–9569.



- [6] M. N. Rosenbluth, H. L. Berk, I. Doxas, W. Horton, *Phys. Fluids* **1987**, *30*, 2636.
- [7] A. M. Soward, *J. Fluid Mech.* **1987**, *180*, 267–295.
- [8] B. I. Shraiman, *Phys. Rev. A* **1987**, *36*, 261.
- [9] W. Young, A. Pumar, Y. Pomeau, *Phys. Fluids* **1989**, *1*, 462.
- [10] T. H. Solomon, J. P. Gollub, *Phys. Fluids* **1988**, *31*, 1372.
- [11] T. H. Solomon, I. Mezić, *Nature (London)* **2003**, *425*, 376–380.
- [12] Y.-N. Young, M. J. Shelley, *Phys. Rev. Lett.* **2007**, *99*, 058303.
- [13] Q. Yin, Y. Li, F. Marchesoni, T. Debnath, P. K. Ghosh, *Phys. Fluids* **2020**, *32*, 092010.
- [14] S. Jiang, S. Granick (Eds.), *Janus particle synthesis, self-assembly and applications* (RSC Publishing, Cambridge, 2012).
- [15] A. Walther, A. H. E. Müller, *Chem. Rev.* **2013**, *113*, 5194–5261.
- [16] M. C. Marchetti, J. F. Joanny, S. Ramaswamy, T. B. Liverpool, J. Prost, M. Rao, R. A. Simha, *Rev. Mod. Phys.* **2013**, *85*, 1143.
- [17] J. Elgeti, R. G. Winkler, G. Gompper, *Rep. Progr. Phys.* **2015**, *78*, 056601.
- [18] C. Torney, Z. Neufeld, *Phys. Rev. Lett.* **2007**, *99*, 078101.
- [19] Y. Li, L. Li, F. Marchesoni, D. Debnath, P. K. Ghosh, *Phys. Rev. Res.* **2020**, *2*, 013250.
- [20] P. K. Ghosh, F. Marchesoni, Y. Li, F. Nori, *Phys. Chem. Chem. Phys.* **2021**, *23*, 11944–11953.
- [21] R. B. Bird, W. E. Stewart, E. N. Lightfoot, *Transport phenomena* (New York, John Wiley & Sons, 2007).
- [22] Y. Min, M. Akbulut, K. Kristiansen, Y. Golan, J. Israelachvili, *Nat. Mater.* **2008**, *7*, 527.
- [23] M. A. Boles, M. Engel, D. V. Talapin, *Chem. Rev.* **2016**, *116*, 11220.
- [24] J. Bialké, T. Speck, H. Löwen, *Phys. Rev. Lett.* **2012**, *108*, 168301.
- [25] Y. Fily, M. C. Marchetti, *Phys. Rev. Lett.* **2012**, *108*, 235702.
- [26] G. S. Redner, M. F. Hagan, A. Baskaran, *Phys. Rev. Lett.* **2013**, *110*, 055701.
- [27] Y. Li, Y. Zhou, F. Marchesoni, P. K. Ghosh, *Soft Matter* **2022**, *18*, 4778–4785.
- [28] P. Tabeling, *Phys. Rep.* **2002**, *362*, 1.
- [29] A. Zoettl, H. Stark, *Phys. Rev. Lett.* **2012**, *108*, 218104.
- [30] R. Rusconi, J. S. Guasto, R. Stocker, *Nat. Phys.* **2014**, *10*, 212–217.
- [31] K. Qi, H. Annepu, G. Gompper, R. G. Winkler, *Phys. Rev. Res.* **2020**, *2*, 033275.
- [32] H. Stommel, *J. Mar. Res.* **1949**, *8*, 24–29.
- [33] M. R. Maxey, *Phys. Fluids* **1987**, *30*, 1915.
- [34] J. D. Weeks, D. Chandler, H. C. Andersen, *J. Chem. Phys.* **1971**, *54*, 5237.
- [35] P. K. Ghosh, Y. Li, G. Marchegiani, F. Marchesoni, *J. Chem. Phys.* **2015**, *143*, 211101.
- [36] D. Debnath, P. K. Ghosh, Y. Li, F. Marchesoni, B. Li, *Soft Matter* **2016**, *12*, 2017–2024.
- [37] A. Zöttl, H. Stark, *J. Phys. Condens. Matter* **2016**, *28*, 253001.
- [38] P. K. Ghosh, V. R. Misko, F. Marchesoni, F. Nori, *Phys. Rev. Lett.* **2013**, *110*, 268301.
- [39] P. E. Kloeden, E. Platen, *Numerical Solution of Stochastic Differential Equations* (Springer, Berlin, 1992).
- [40] Y. Li, Q. Yin, F. Marchesoni, T. Debnath, P. K. Ghosh, *Phys. Rev. E* **2021**, *103*, L030106.
- [41] Y. Li, P. K. Ghosh, F. Marchesoni, *Phys. Rev. Res.* **2021**, *3*, L032065.
- [42] M. E. Cates, J. Tailleur, *Annu. Rev. Condens. Matter. Phys.* **2015**, *6*, 219–244.
- [43] T. Kolbab, D. Klotsa, *Soft Matter* **2020**, *16*, 1967–1978.
- [44] J. Stürmer, M. Seyrich, H. Stark, *J. Chem. Phys.* **2019**, *150*, 214901.
- [45] J. Agudo-Canalejo, R. Golestanian, *Phys. Rev. Lett.* **2019**, *123*, 018101.
- [46] P. Dolai, A. Simha, S. Mishra, *Soft Matter* **2018**, *14*, 6137–6145.
- [47] W. Yang, V. R. Misko, F. Marchesoni, F. Nori, *J. Phys. Condens. Matter* **2018**, *30*, 264004.
- [48] X. Yang, M. L. Manning, M. C. Marchetti, *Soft Matter* **2014**, *10*, 6477–6484.
- [49] J. Stenhammar, R. Wittkowski, D. Marenduzzo, M. E. Cates, *Phys. Rev. Lett.* **2015**, *114*, 018301.
- [50] A. Wysocki, R. G. Winkler, G. Gompper, *New J. Phys.* **2016**, *18*, 123030.
- [51] K. C. Leptos, J. S. Guasto, J. P. Gollub, A. I. Pesci, R. E. Goldstein, *Phys. Rev. Lett.* **2009**, *103*, 198103.
- [52] D. Debnath, P. K. Ghosh, V. R. Misko, Y. Li, F. Marchesoni, F. Nori, *Nanoscale* **2020**, *12*, 9717–9726.
- [53] J. Elgeti, G. Gompper, *EPL* **2013**, *101*, 48003.
- [54] Y. Fily, Y. Kafri, A. P. Solon, J. Tailleur, A. Turner, *J. Phys. A* **2018**, *51*, 044003.
- [55] S. Das, G. Gompper, R. G. Winkler, *Sci. Rep.* **2019**, *9*, 6608.
- [56] R. Matas-Navarro, R. Golestanian, T. B. Liverpool, S. M. Fielding, *Phys. Rev. E* **2014**, *90*, 032304.
- [57] M. Theers, E. Westphal, K. Qi, R. G. Winkler, G. Gompper, *Soft Matter* **2018**, *14*, 8590–8603.
- [58] N. Korin, M. Kanapathipillai, B. D. Matthews, M. Crescente, A. Brill, T. Mammoto, K. Ghosh, S. Jurek, S. A. Bencherif, D. Bhatta, A. U. Coskun, C. L. Feldman, D. D. Wagner, D. E. Ingber, *Science* **2012**, *337*, 738–42.
- [59] M. J. Gomez-Garcia, A. L. Doiron, R. R. M. Steele, H. I. Labouta, B. Vafadar, R. D. Shepherd, I. D. Gates, D. T. Cramb, S. J. Childs, K. D. Rinker, *Nanoscale* **2018**, *10*, 15249–15261.
- [60] M. F. Attia, N. Anton, J. Wallyn, Z. Omran, T. F. Vandamme, *J. Pharm. Pharmacol.* **2019**, *71*, 1185–1198.

---

Manuscript received: July 4, 2022

Revised manuscript received: September 19, 2022

Accepted manuscript online: September 20, 2022

Version of record online: October 25, 2022